Developmental Biology 341 (2010) 315–323

Contents lists available at ScienceDirect

Developmental Biology

journal homepage: www.elsevier.com/developmentalbiology

Evolution of Developmental Control Mechanisms

Evolution of oropharyngeal patterning mechanisms involving *Dlx* and *endothelins* in vertebrates

Shigehiro Kuraku [a,*,1], Yoko Takio [a,1], Fumiaki Sugahara [a,b], Masaki Takechi [a], Shigeru Kuratani [a]

[a] *Laboratory for Evolutionary Morphology, RIKEN Center for Developmental Biology, 2-2-3 Minatojima-minami, Chuo-ku, Kobe 650-0047, Japan*
[b] *Graduate School of Science, Kobe University, Kobe 657-8501, Japan*

ARTICLE INFO

Article history:
Received for publication 1 January 2010
Revised 5 February 2010
Accepted 6 February 2010
Available online 18 February 2010

Keywords:
Lamprey
Jaw
Pharyngeal arch
Dlx-code
Endothelin

ABSTRACT

In jawed vertebrates, the Dlx code, or nested expression patterns of *Dlx* genes, specify the dorsoventral polarity of pharyngeal arches, downstream of *endothelin-1* (*Edn-1*) and its effectors, *Bapx1* (*Nkx3.2*) and *dHand* (*Hand2*). To elucidate the evolution of the specification mechanism of the oropharyngeal skeletal system, lamprey homologs of *Dlx*, *Edn*, *endothelin receptor* (*Ednr*), *Bapx1*, and *dHand* were identified. Our analysis suggested that the *Edn* gene family emerged at the advent of vertebrates, and that gene duplications leading to the different *Edn* gnathostome subtypes (*Edn1–3*) occurred before the cyclostome–gnathostome split. This timing of gene duplications, giving rise to multiple subtypes, was also implied for *Dlx*, *Ednr*, *Hand*, and *Bapx*. In lamprey embryos, nested expressions of *Dlx* genes were not observed in pharyngeal arches, nor was any focal expression of *Bapx1*, known in gnathostomes to specify the jaw joint. The *dHand* homolog, however, was expressed more intensively ventrally, as in gnathostomes. Lamprey homologs of *Edn-1* and *EdnrA* were also shown to be expressed as described in mice, indicating involvement of this signaling pathway in the craniofacial patterning early in vertebrate evolution. These results suggest that the last common ancestor of all the extant vertebrates would have possessed basic gene repertoires involved in oropharyngeal patterning in gnathostomes, but the elaborate genetic program leading to the Dlx code is likely to have been acquired uniquely in gnathostomes.

Introduction

Living agnathans (jawless vertebrates) contain two extant members (hagfishes and lampreys) that are categorized into Cyclostomata (summarized in Kuraku, 2008). For the evolution of the jaw, dorsoventral division of the embryonic mandibular arch as well as specification of upper and lower moieties are prerequisite developmentally (reviewed in Kuratani and Ota, 2008; Mallatt, 2008). Consistent with the apparent lack of this division, the posterior pharyngeal arches (PAs3–9) in the lamprey exhibit dorsoventrally symmetrical patterns (Supplementary Fig. 1; Yao et al., 2008). To elucidate the evolution of the feeding apparatus, lampreys thus provide important clues with which to better understand the evolution of oropharyngeal patterning at molecular and developmental levels (Kuratani et al., 2002; Shigetani et al., 2002).

In the mouse, the anteroposterior specification of PAs is regulated by the Hox code, in which the mandibular arch is defined by the absence of the *Hox* transcripts (*Hox*-free default state; Hunt et al., 1991; Rijli et al., 1993), whereas the dorsoventral specification is regulated by the nested expression patterns of *Dlx* genes (Dlx code); in the mandibular arch, *Dlx5* and *-6* are expressed only in the ventral half to specify the mandibular identity (Depew et al., 2002). The craniofacial patterning of the gnathostomes is now generally thought to depend on the Cartesian patterns of Hox/Dlx codes that provide specific combinations of homeobox genes' transcripts in each part of the neural crest-derived ectomesenchyme. The lamprey has been shown to express some *Hox* genes in the PAs and the neural tube in patterns partly similar to those in gnathostomes (jawed vertebrates), including the *Hox*-free default state of the mandibular arch (Takio et al., 2007, 2004).

The *Dlx* subfamily of homeobox-containing genes has experienced a series of tandem and chromosomal duplications (Stock et al., 1996; Panganiban and Rubenstein, 2002). Non-teleost gnathostomes surveyed so far generally possess six genes (*Dlx1–6*; Stock, 2005), while teleosts have gained additional paralogs in the teleost-specific genome duplication (Debiais-Thibaud et al., 2008). Four *Dlx* genes have been reported so far in the sea lamprey *Petromyzon marinus* (Neidert et al., 2001), all of which are expressed in the PAs. It has not yet been determined, however, whether the Dlx code exists. Recently, six *Dlx* genes including orthologs of the above four have been reported for the Japanese lamprey *Lethenteron japonicum* (Kuraku et al., 2009). Thus, there remain two lamprey *Dlx* genes that have not been well characterized.

* Corresponding author. Present address: Laboratory for Zoology and Evolutionary Biology, Department of Biology, University of Konstanz, Universitätsstrasse 10, 78464 Konstanz, Germany. Fax: +49 7531 88 3018.
E-mail address: shigehiro.kuraku@uni-konstanz.de (S. Kuraku).
[1] These authors equally contributed to this work.

0012-1606/$ – see front matter © 2010 Elsevier Inc. All rights reserved.
doi:10.1016/j.ydbio.2010.02.013

Recent studies in mouse and zebrafish have shown that expression of *Dlx* genes in PAs is regulated by *endothelin-1* (*Edn-1*; *sucker* in zebrafish; Kimmel et al., 2003). *Edn-1* encodes a precursor peptide, whose mature signal is recognized by endothelin receptors (Ednr; Hyndman et al., 2009) and mediated by a homeobox-containing gene *Bapx1* (*Nkx3.2*) and a helix–loop–helix motif-containing gene *dHand* (*Hand2*) (Miller et al., 2003). Among the members of the *Edn* gene family, only *Edn-1* has been functionally characterized in the craniofacial patterning (e.g. Sato et al., 2008). In addition to the origin of this gene, whose homologs have never been reported for invertebrates, this gene family provides intriguing questions as to the timing of gene duplications that gave rise to three *Edn* paralogs. The same line of analysis should shed light on relationships between evolution of repertoires of *Dlx* and other related genes, and establishment of the jaw patterning program.

In this study, we identified cDNAs of *Dlx*-, *Edn*-, *Ednr*-, *Bapx*-, and *Hand* homologs in *L. japonicum* and analyzed their expression patterns to better understand the evolution of mechanisms that have resulted in the remarkable diversity of the vertebrate pharyngeal skeleton. Our results suggest that the vertebrate common ancestor would have already had basic gene repertoires possessed by gnathostomes, but that the Dlx code is likely to have been obtained in the gnathostomes, which would have led to the acquisition of the dorsoventrally articulated jaw.

Results

Identification of Dlx, Edn, Ednr, Bapx and Hand homologs in the lamprey

L. japonicum possesses at least six Dlx genes (designated *LjDlxA–F* [AB292628–AB292633]; Kuraku et al., 2009). The one that used to be designated *LjDlx1/6* (AB048759; Murakami et al., 2001; Myojin et al., 2001; Neidert et al., 2001) has been renamed *LjDlxD* (AB292631), an ortholog of *P. marinus DlxD* (AY010119).

For *L. japonicum*, we isolated cDNAs of homologs of *endothelin receptor type A* (*EdnrA*), *Bapx1* and *dHand*, designated *LjEdnrα* (AB537175), *LjBapxA* (AB293607) and *LjHandA*, (AB293608), respectively. We also isolated six cDNAs encoding *Edn* homologs, designated *LjEdn-A*, *-B*, *-C*, *-D*, *-E* and *-F* (AB293609–AB293614). We did not detect any further sequence with apparent homology to the genes of interest in partial *P. marinus* genome sequences.

Molecular phylogeny of the lamprey Dlx, Edn, Ednr, Bapx and Hand

The molecular phylogeny of the lamprey *Dlx* genes has been discussed previously (Kuraku et al., 2009; Neidert et al., 2001). The former, based on more sophisticated methodology, produced extremely low supports for groupings of gnathostome orthologs *per se* (*Dlx1–6*), and for the positions of *LjDlx* genes. However, the analysis explicitly supported close relationships of *LjDlxA*, *-B*, and *-C* with the gnathostome *Dlx2/3/5* subgroup, and *LjDlxD*, *-E*, and *-F* with the gnathostome *Dlx1/4/6* subgroup (Supplementary Figs. 2A and B; see also Supplementary Text).

Of the six *L. japonicum Edn* homologs, we obtained relatively long cDNA sequences for only *LjEdn-A* and *-E* (Supplementary Fig. 3A). In spite of exhaustive *in silico* searches in diverse organisms outside Vertebrata, we found no sequences significantly similar to any known *Edn* gene. Thus, the lamprey *Edn* genes identified in this study are likely to represent the most early-branching homologs of this gene family. Our analysis detected conserved macrosynteny between human chromosomes 1, 6, and 20, each of which has a single *Edn* paralog (Supplementary Fig. 4B; see Kuraku et al., 2009) for details of the method; also see Braasch et al., 2009 for conserved syntenies among teleost fish genomes). This clearly shows that these gene duplications are part of large-scale duplications. Our unrooted phylogenetic tree of *Edn* genes, based on an extremely short residue stretch (58 amino acids), reconstructed groupings of gnathostome *Edn-2* (bootstrap probability, 26%) and *Edn-3* (bootstrap probability, 67%), between which relationships within gnathostome *Edn-1* are not properly reconstructed (Supplementary Fig. 4A). The tree, however, showed the closest relationship of *LjEdn-A* to gnathostome *Edn-1*, while *LjEdn-E* was relatively closely related to gnathostome *Edn-3* (Supplementary Fig. 4A). Positions of *LjEdn-B*, *-C*, *-D*, and *-F* were also inferred with shorter alignment lengths but were not supported with high confidence (Supplementary Fig. 4A).

Our *LjEdnrα* contained most of conserved amino acid residues shared among vertebrate Ednr genes. Using the amphioxus *Ednr*-like gene as an outgroup, we obtained the ML tree supporting an orthology of the *LjEdnrα* to the jawed vertebrate *EdnrA* subtype (bootstrap probabilities in ML and NJ, 97 and 85, respectively; Supplementary Fig. 5A). All tree topologies placing the *LjEdnrα* gene at the basal branch of three vertebrate subtypes, *EdnrA*, *EdnrB1* and *EdnrB2* were strongly rejected within the 1SE of log-likelihood. Short alignments of *LjBapxA* and *LjHandA* did not provide high resolution (Supplementary Figs. 5B and C; Supplementary Table 2). However, our probabilistic analysis supported orthologies of *LjBapxA* and *LjHandA* to gnathostome *Bapx1* and *dHand*, respectively (bootstrap probabilities in ML, 68 and 94).

Expression analysis of lamprey Dlx genes

To gain insights into the evolution of the oropharyngeal patterning program, we observed expressions of the genes described above, especially in the craniofacial regions of the *L. japonicum* embryo during morphogenetic stages, by whole-mount *in situ* hybridization and sectioning of stained embryos.

Expression of *LjDlxA* started at stage 22 in the rostral ectoderm including the future nasohypophysial plate (Supplementary Fig. 6A). By stage 26, *LjDlxA* had become highly upregulated in the ectoderm and ectomesenchyme of the upper and lower lips, as well as in the velum (Fig. 1A), in contrast to a previous report (Neidert et al., 2001). Lower levels of expression were also seen in the ectomesenchyme of the velum and more posterior PAs (Fig. 1B). Expression was also detected in the otocyst and the forebrain (striatum and thalamus; Fig. 1B). Throughout the developmental stages examined, there was no overt dorsoventral gradient of *LjDlxA* expression in the PAs (Fig. 1B).

Spatiotemporal expression patterns of *LjDlxC*, *-D*, and *-E* were very similar to those of *LjDlxA*; these were detected in the rostral surface ectoderm, otic pit or otocysts, ectodermal and ectomesenchymal components of the oral apparatus, and PA ectomesenchyme (Figs. 1F, H, and J; Supplementary Text). Again, the upregulation in the oropharyngeal ectomesenchyme proceeded in an anterior to posterior direction, with no clear difference detected in the intensity of expression along the dorsoventral axis of the PAs (Figs. 1F, H, and J). Also, by our *in situ* hybridization, expressions of *DlxA*, *-C*, and *-D* were weakly detected in migrating crest cells (e.g. Fig. 1M for *LjDlxC*), as reported previously for their homologs in *Petromyzon marinus* (Neidert et al., 2001).

Expression of *LjDlxB* was slightly different from the above paralogs. Its transcripts were first observed at stage 22, when a low level of *LjDlxB* transcripts were detected in the ectoderm of the cheek process as well as in the putative cephalic crest cells (Supplementary Figs. 6C and D). Previously, expression signals in migrating crest cells was not described for *P. marinus DlxB* (Neidert et al., 2001). Stronger expression was observed after stage 25 in the craniofacial ectomesenchyme as other genes (Figs. 1C and D), however, no expression was found in the forebrain.

LjDlxF is peculiar in that it is expressed almost exclusively in the olfactory placode at stage 22–24 (Supplementary Fig. 6H) and the velothyroideus muscle at stage 26 (Fig. 1L; Supplementary Figs. 6I and J; see Holland et al., 1993). No clear ectomesenchymal expression for this gene was detected.

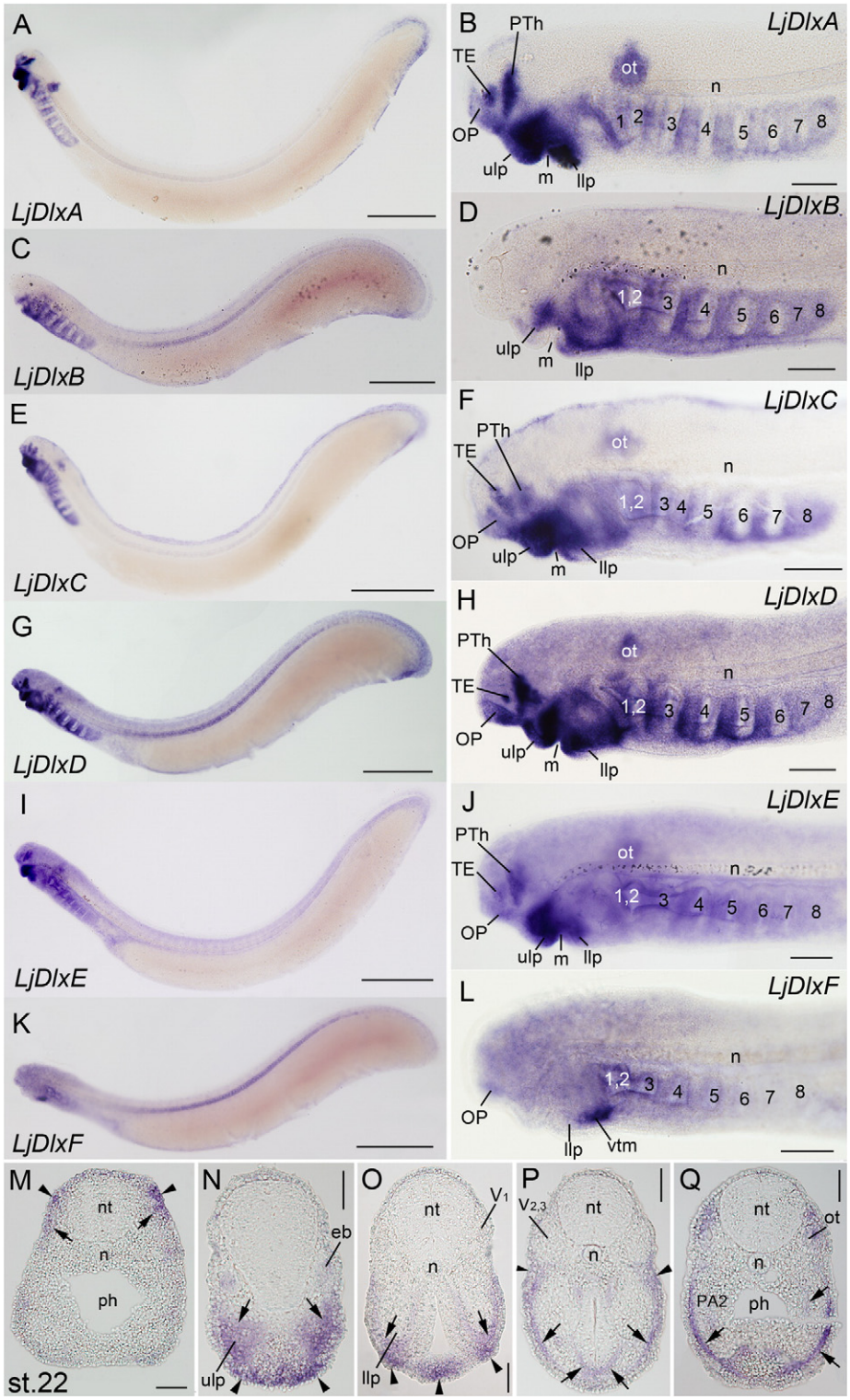

Fig. 1. Expression patterns of the lamprey *DlxA–F*. (A, C, E, G, I, K) *LjDlxA–F* expression signals stained with *in situ* hybridization at stage 26. (B, D, F, H, J, L) Magnifications of craniofacial region in A–F, respectively. *LjDlxA*, *-C*, and *-D* were expressed in the olfactory placode (OP), telencephalon (TE), prethalamus (PTh), otocyst (ot), upper and lower lips (ulp and llp), and neural crest-derived ectomesenchyme in the PAs (B, F, and H). *LjDlxB* transcripts were detected in the ulp, llp, and ectomesenchyme in the PAs (D). *LjDlxE* was expressed in the telencephalon, prethalamus, otocyst, and upper and lower lips (J). *LjDlxF* transcripts were detected in the olfactory placode and velothyroideus muscle (vtm) (L). (M–Q) Histological observations of *LjDlxC* expression. (M) A transverse section to show the expression in migrating neural crest cells at stage 22 (arrows) and ectoderm (arrowheads). (N–Q) Transverse sections of a stage 26 larva. Transcripts are detected in the ectomesenchyme (arrows) and ectoderm (arrowheads). eb, eyeball; m, mouth; mc, mesodermal core; n, notochord; nt, neural tube; ph, pharynx; V_1, ophthalmicus profundus nerve; $V_{2,3}$, maxillomandibular nerve; 1–8; pharyngeal pouch 1–8. Scale bars: 0.5 mm in A–F; 0.1 mm in G–L; 0.05 mm in M and N–Q.

Histological observations showed that the *LjDlxC* expression was restricted to the ectomesenchyme, and that the mesodermal cores of the arches were devoid of expression (Fig. 2E). Similar patterns of expression signals were detected for *LjDlxB* and *-D*, while signals in a part of the PA ectomesenchyme medial to the mesodermal core were missing for *LjDlxA* and *-E* (Figs. 2A and I). Expression signals in the

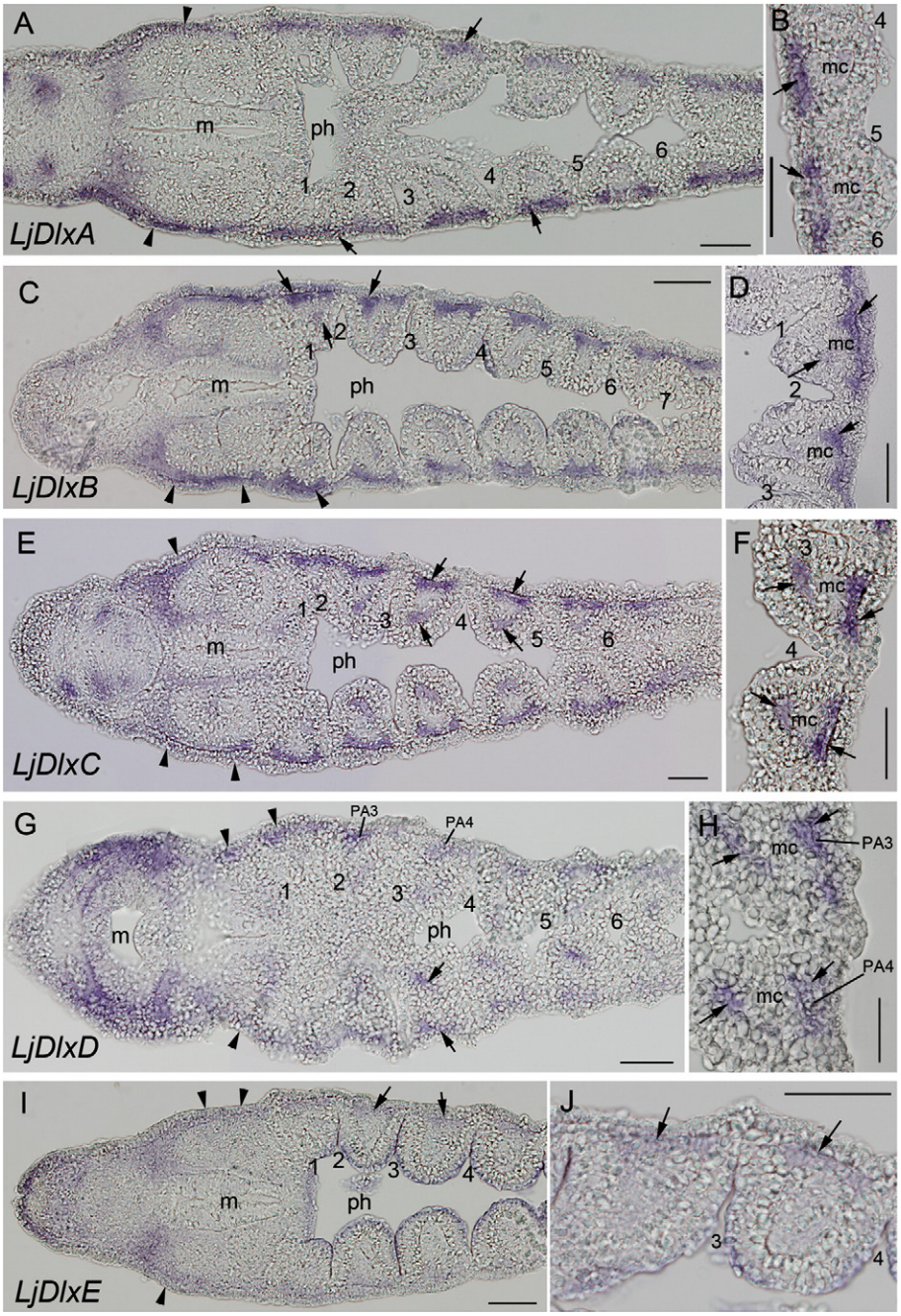

Fig. 2. Craniofacial expressions of the lamprey *DlxA–E* in horizontal sections. (A, B) *LjDlxA*. (C, D) *LjDlxB*. (E, F) *LjDlxC*. (G, H) *LjDlxD*. (I, J) *LjDlxE*. (A, C, E, G, I) Horizontal views for the craniofacial region produced by cryosectioning of *L. japonicum* embryos stained with *in situ* hybridization. (B, D, F, H, J) Magnification of the selected parts in A, C, E, G, and I, respectively. Arrows and arrowheads indicate expression signals in ectomesenchyme and epithelium, respectively. m, mouse; ph, pharynx; mc, mesodermal core; 1–7, pharyngeal pouch; PA, pharyngeal arch. Scale bars: 0.05 mm.

nasohypophysial placode, telencephalon and prethalamus, which were observed for *LjDlxA*, *-C*, *-D* and *-E*, were not detected for *LjDlxB*, whereas, of those, only the signal in nasohypophysial (olfactory) placode was detected for *LjDlxF* (Fig. 1L). Many of the expressions described here persisted until stages 28 or 29 (see Supplementary Figs. 6B, E, G and I).

Expression analysis of lamprey Edn, Ednr, BapxA and HandA genes

During the late pharyngula stages, *LjEdn-A* was upregulated in perioral surface ectoderm and also in the PA ectomesenchyme at lower levels (Figs. 3A–C). In particular, *LjEdn-A* was most strongly expressed in the upper lip ectoderm (Fig. 3D). *LjEdn-C*, on the other hand, was strongly expressed in the lower lip ectoderm (Supplementary Figs. 7A–C). *LjEdn-E* was upregulated only in late stage embryos, in the dorsal part of the upper lip, as well as in the PA mesenchyme (Supplementary Figs. 7D–G).

Expression signals for *LjEdnrα* were first detected at stage 23 in some parts of developing brain, upper and lower lips, pharyngeal arches and heart (Supplementary Fig. 8A), and these persisted even at stage 26 (Fig. 3G). At stage 23, this gene was also expressed in the migrating neural crest cells and ectomesenchyme beneath the ectoderm in the cheek process (Supplementary Fig. 8B). In transverse sections, transcripts were detected in the ectomesenchyme of the upper lip (Fig. 3H), and the ectomesenchyme as well as epithelium beneath the pharyngeal endoderm in the lower lip and posterior arches (Figs. 3I–L).

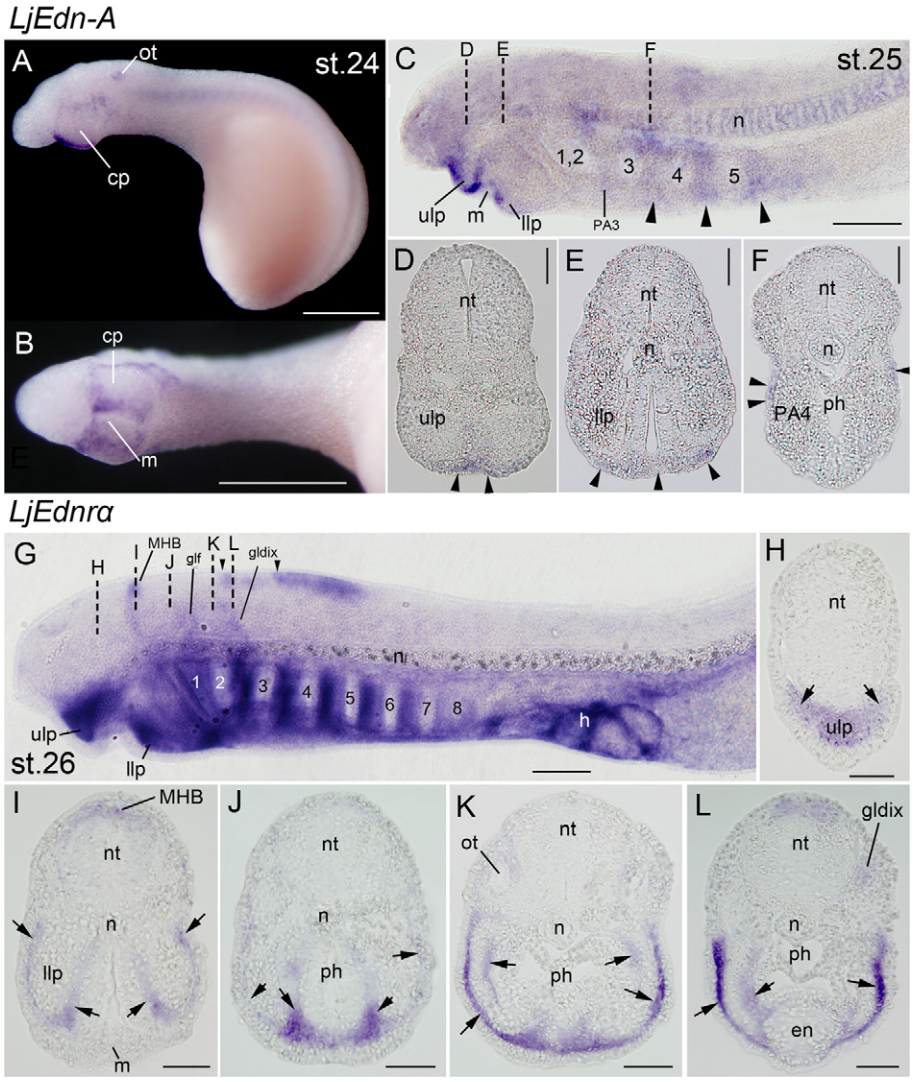

Fig. 3. Expression patterns of the lamprey *Edn* and *Ednr* homologs. (A) Lateral view of *LjEdn-A* expression at stage 24. (B) Ventral view of the embryo shown in A. *LjEdn-A* was expressed in the otocyst (ot) and surface ectoderm around the cheek process (cp). (C) *LjEdn-A* expression in the craniofacial region at stage 25. Transcripts were detected in the upper (ulp) and lower lips (llp), and ectomesenchyme in the PAs (arrowheads). (D–F) Transverse sections of the embryo shown in C at each anteroposterior levels. (G) *LjEdnrα* expression at stage 26. Judging from positioning of pharyngeal arches, expression in the hindbrain resided in rhombomeres 4–6 (arrowheads) (see Takio et al., 2007). Expression signals were also observed in the midbrain–hindbrain boundary (MHB), ganglion of facial nerve (glf), ganglion of glossopharyngeal nerve (gldix) (see Kuratani et al., 1997), pharyngeal arches 1–8, heart (h). (H–L) Transverse sections of the embryo at anteroposterior levels shown in G. h, heart; m, mouth; n, notochord; nt, neural tube; ph, pharynx; en, endostyle; 1–8, pharyngeal pouch 1–8. Scale bars: 0.5 mm in A and B; 0.1 mm in C and G; 0.05 mm in D–F and H–L.

Transcripts of the *LjHandA* gene were first detected in the ventral midline of the oropharyngeal region (Fig. 4A), except at the level at which the endostyle arises (Fig. 4C). At stage 26, the expression signal persisted in the ventral region (Fig. 4D) and was mostly in the subepidermal mesenchyme, probably derived from the neural crest (Figs. 4E and F). Two major expression domains were detected for *LjBapxA*; namely, the trigeminal nerve ganglion (Figs. 4G and H) and a domain in the ectoderm of the mandibular arch (Figs. 4H and I). The latter domain corresponded to the boundary between the lower lip and the velum of the larva (Fig. 4H).

Discussion

Molecular phylogeny of cyclostome genes

Gene repertoires in vertebrate genomes have been shaped by a series of whole genome duplications (WGDs) and also successive, small-scale gene gains and losses. It has been pointed out that molecular phylogenies of cyclostome genes tend to provide low resolution in interpreting the timing of WGDs (Kuraku, 2008). Thus, it is inevitable that genes with short alignments, like those in this study, cannot provide sufficient resolution. A genome-wide view is the key to addressing this difficult question.

Our analysis of the human chromosomes has shown that members of the *Edn* gene family were duplicated in chromosomal, or WGDs, probably before the cyclostome–gnathostome split (Supplementary Fig. 4A; Fig. 5). It is suggested that *Bapx* and *Hand* gene families, whose members are localized on the human chromosomes 4, 5, and 8, expanded through the same event (Wotton et al., 2008), which also holds true for the *Dlx* family (Larhammar et al., 2002). The present phylogenetic analysis involving the *Pdk* gene family, linked tightly with *Dlx* gene clusters (Supplementary Fig. 2; Supplementary Text), provided still unresolved, but uniform evidence of redundant gene repertoires in the lamprey: more gene duplications were observed before the cyclostome–gnathostome split than after (Fig. 5). The phylogeny of a lamprey endothelin receptor homolog *LjEdnrα* clearly indicated that it is orthologous to only the jawed vertebrate *EdnrA* subtype, and that gene duplications, giving rise to multiple subtypes, preceded the cyclostome–gnathostome split (Supplementary Fig. 5A; Supplementary Table 2). This is consistent with the recently proposed

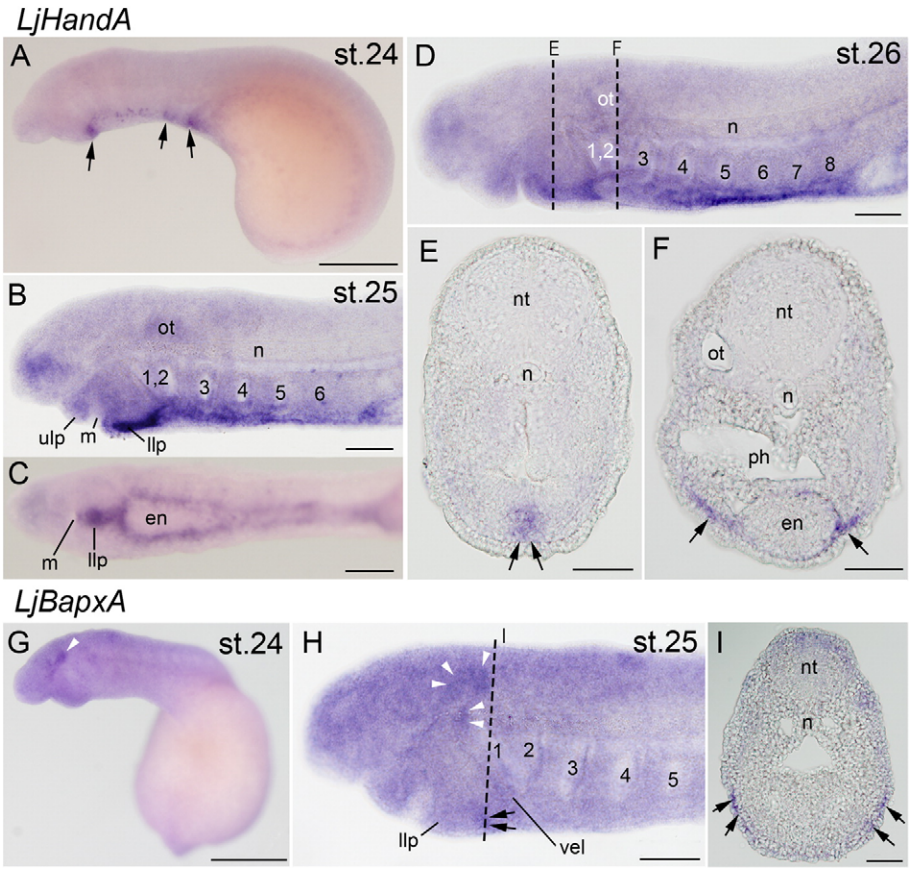

Fig. 4. Expression patterns of the lamprey *Bapx1* and *dHand* homologs. (A) *LjHandA* expression at stage 24 (arrows). (B) *LjHandA* expression at stage 25. (C) Ventral view of the embryo in B. (D) *LjHandA* expression at stage 26. (E, F) Transverse sections at the level anterior to the PA1 and the level in the PA3 shown as dotted lines in I, respectively. *LjHandA* was expressed in the ectomesenchyme in the PAs (arrowheads in E and F) on the ventral part of oropharyngeal region except the endostyle (en). (G) *LjBapxA* expression at stage 24. (H) *LjBapxA* expression at stage 25. (I) Transverse section at the level shown as a dotted line in H. Transcripts were detected in the trigeminal nerve ganglion (white arrowheads in G and H), and a domain in the ectoderm of the mandibular arch (black arrows in H). m, mouth; n, notochord; nt, neural tube; ph, pharynx; 1–8, pharyngeal pouch 1–8; vel, velum. Scale bars: 0.5 mm in A and G; 0.1 mm in B, C, D, and H; 0.05 mm in E, F, and I.

hypothesis based on large-scale phylogenetic analysis using longer genes (Kuraku et al., 2009).

Edn signaling: invention in Vertebrata

Among the gene families analyzed, the *Edn* gene family is uniquely devoid of invertebrate homologs. The most parsimonious explanation is that the ancestral gene of this gene family should have emerged in the vertebrate lineage (Fig. 5). Our analysis detected expression signals in the oral region not only for *LjEdn-A*, a possible ortholog for gnathostome *Edn-1* (Figs. 3A–F), but also for *LjEdn-C* and *-E* (Supplementary Fig. 7), both of which are relatively closely related to gnathostome *Edn-3* (Supplementary Fig. 4A). So far, no studies have described *Edn-3* expression in oral regions, although implicated in the differentiation of neural crest cells (Nataf et al., 1996): this gene has been characterized mainly in the context of melanocyte differentiation (e.g. Thomas and Erickson, 2008). If we regard this as a lack of gnathostome *Edn-3* expression in the oral region, our observation of *LjEdn-C* and *-E* expression suggests that the ancestral *Edn* gene would have exhibited oral expression, which was secondarily lost from the *Edn-3* specifically in the gnathostome lineage (Fig. 5). It is possible that this group of genes primarily took a pivotal role in oropharyngeal patterning, which led to the acquisition of the jaw through a secondary modification of expression patterns.

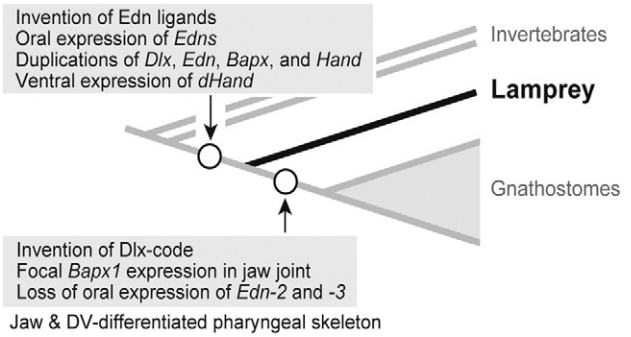

Fig. 5. A hypothesized scenario for evolution of molecular mechanisms that gave rise to the jaw apparatus.

In mice, *EdnrA* is expressed in neural crest-derived ectomesenchymal cells (Kurihara et al., 1994, 1995; Clouthier et al., 1998). *LjEdnrα*, its possible lamprey ortholog (Supplementary Fig. 5A), has been shown to be expressed in their corresponding areas in pharyngeal arches (Fig. 3G–L). This gene was found also to be expressed in some portions of central nervous system, including the hindbrain, and the heart (Fig. 3G; Supplementary Fig. 8). The heart expression is described for mouse *EdnrA* (Clouthier et al., 1998). In the neural tube, however, in the quail, Edn-signaling is achieved with a paralogous set of genes, namely *Edn3* and *EdnrB1* (Nataf et al., 1996). Whether the CNS-associated expression of *LjEdnrα* suggests a lineage-specific reshuffling of expression domains or reflects an ancestral organization between paralogs should further be examined by characterizing other paralogs of cyclostomes, if any. A high level of similarity in expression patterns between the lamprey and

mouse was observed also for *LjEdn-A* and *Edn1* genes: both are expressed in the epithelium of the anterior pharyngeal arches (Fig. 3A–D; Maemura et al., 1996). This implies that Edn-signaling mediated by the *EdnrA* cognate would have already been established before the split between cyclostomes and gnathostomes, playing patterning roles in craniofacial development.

Evolution of Dlx genes and Dlx code

Our previous study suggested a lineage-specific gene duplication between *LjDlxA* and *-C* (Kuraku et al., 2009), which denies the orthologies of each of six *LjDlx* genes to one of six gnathostome *Dlx* subtypes. However, relationships within each gnathostome Dlx subtype were not reconstructed unambiguously or with high confidence (e.g., polyphyly of *Dlx4*; Supplementary Figs. 2A and B). The structure of *Dlx* gene clusters in the lamprey, if any, should add more clues about orthologies of *LjDlx* genes. Below, we discuss *Dlx* gene expression in lampreys and gnathostomes based on the idea that they have a similar level of redundancy in *Dlx* gene repertoires.

The most curious implication in our present study was that the Dlx code may not have been present in the earliest phase of vertebrate evolution (Figs. 1 and 5; see Fig. 6 for a summarized scheme of craniofacial *Dlx* expressions). Gnathostome PA skeletons, especially those of the mandibular arch, are characterized by morphologically well differentiated dorsoventral moieties. Namely, the upper jaw and lower jaw elements are distinctly different from each other to fulfill mechanical movements as well as for their integration with other parts of the skull. Thus, the cartilaginous element of the gnathostome upper jaw is called the palatoquadrate and is composed of specific sets of subdivisions (reviewed in Moore, 1981). In the lamprey, in contrast, the wireframe-like branchial arch cartilage shows a dorsoventrally symmetrical configuration both in the ammocoete larvae and in the adult (Supplementary Fig. 1). This, however, does not necessarily mean that the lamprey PAs lack any sign of dorsoventral specification. The lamprey mandibular arch differentiates into the velar and lower lip cartilage that does not appear dorsoventrally symmetrical (reviewed in Kuratani et al., 2001; Shigetani et al., 2005). Furthermore, the mandibular arch skeleton of the adult lamprey as well as of the hagfish has differentiated into the highly elaborate morphology of the cyclostome-specific 'tongue' in the ventral oral cavity (Kuratani and Ota, 2008; Yalden, 1985). Thus, as far as the mandibular arch-derivatives are concerned, the cyclostome PA is morphologically differentiated dorsoventrally. Consistently, the *LjHandA* expression is restricted in the ventral part of the lamprey pharynx (Figs. 4B and D), suggesting that there would also be dorsoventral specification programs in the lamprey, independent of the Dlx code. Alternatively, the timing of *Dlx* transcription, which takes place ventrally and slightly earlier, may possibly lead to such a specification.

It remains enigmatic how and in which sequence the gnathostomes have acquired dorsoventrally articulated and differentiated oral apparatus in the mandibular arch. It has been suggested that possession of paired nostrils (diplorhiny) and posterior shift (heterotopy) of FGF/BMP signaling were prerequisites for the gnathostome-type jaws (Shigetani et al., 2002; reviewed in Kuratani, 2005; Kuratani and Ota, 2008; also see Mallatt, 2008). The latter changes are likely to have been obtained after the split of cyclostome and gnathostome lineages. This timing seems to be also the case for the establishment of the Dlx code and focal expression of *Bapx1* in the jaw joint (Wilson and Tucker, 2004; Fig. 5).

Doubtlessly, establishment of a dorsoventral hinge should have been a critical event for jaw evolution. It is suggested that the *Edn*-dependent signaling prefigured the *Bapx1* regulation as well as the establishment of the Dlx code (Miller et al., 2003). Consistently, there is little dorsoventral differentiation of the gnathostome jaw in basal groups such as acanthodians (Koentges and Matsuoka, 2002). However, it should be pointed out that, in placoderms and chondrichthyes, the upper and lower jaws are already well differentiated morphologically (Janvier, 1996), implying a fully functional Dlx code. In this context, it would be intriguing to evaluate the morphological patterns of PA skeletons in the jawless, stem groups of gnathostomes, collectively known as the ostracoderms (Janvier, 1996). Even if they lacked the jaw, their PA skeleton may have shared with gnathostomes certain Dlx code-dependent dorsoventral patterns absent from cyclostomes.

Another puzzling question is the apparently redundant expression of the *Dlx* genes in the lamprey (Fig. 6). A possibility is that the *Dlx* genes function during lamprey metamorphoses. In this connection, it would be interesting to know expression patterns of *Dlx* genes in the hagfishes, which directly develop a mandibular arch-derived tongue apparatus in their embryonic development (Ota et al., 2007).

Materials and methods

Animals

Sources of *L. japonicum* embryos were described previously (Takio et al., 2007). Embryonic staging was based on (Tahara, 1988). Total RNA of *L. japonicum* was extracted from whole embryos at stages 20, 24, 28, and 30.

cDNA cloning and sequencing

Basic procedures from cDNA synthesis to sequencing were described previously (Kuraku et al., 2008). For *Edn* genes, the sense degenerate primers 5′-GAC AAG GAR TGY RTN TAY TWY TGY CAY-3′ and 5′-C TTC TGT CAC YTN GAY RTN RTN TGG -3′ were designed based on amino acid residues, DKECVYYCH and YYCHLDIIW, respectively. For the *LjBapxA* gene, the sense degenerate primers 5′-GAG ACN CAR GTN AAR ATH TGG TTY CA-3′ and 5′-TTC CAG AAC MGN MGN TAY AAR ACN AA -3′ were designed based on amino acid residues, ETQVKIWFQ and FQNRRYKTK, respectively. For the *LjEdnrα* gene, the sense degenerate primer 5′-TGG CTG TTY GGC TTY TAY TT-3′ and the antisense primer 5′-AR CGC NAT NGG RTT NAT RCA-3′ were designed based on amino acid residues, WLFGFYF and SINPIAL, respectively. For the *LjHandA*, we used primers designed based on the nucleotide sequence of a putative *P. marinus* ortholog found in genome traces, namely, 5′-CTACATCGCCTACCTCATG-3′ and 5′-CTACCTCATG-GAGGTGCT-3′. These primers were used for primary and nested amplification of stretches spanning from their coding regions to the 3′-end. Sequences identified in this study are deposited in GenBank (URL: http://www.ncbi.nlm.nih.gov/Genbank) under accession numbers AB293607–AB293614 and AB537175.

Molecular phylogenetic analysis

Amino acid sequences were retrieved from GenBank, Refseq and Ensembl. We also surveyed partial genome sequences of the sea lamprey *P. marinus* and the elephant shark *Callorhinchus milii* available at Ensembl *Pre!* (http://pre.ensembl.org/Petromyzon_marinus/) and NCBI Genome Survey Sequence (GSS) (Venkatesh et al., 2007), respectively, and expressed sequence tags (ESTs) of the spiny dogfish *Squalus acanthias* and the little skate *Leucoraja erinacea* available at NCBI dbEST. Alignment and preliminary neighbor-joining trees were constructed as described previously (Kuraku et al., 2008). Final phylogenetic trees were inferred with the maximum-likelihood method using PhyML (Guindon and Gascuel, 2003), assuming the $JTT+I+\Gamma_4$ model.

In situ hybridization

We excluded all highly conserved nucleotide stretches (e.g., homeoboxes) to avoid cross-hybridization among paralogs. For each

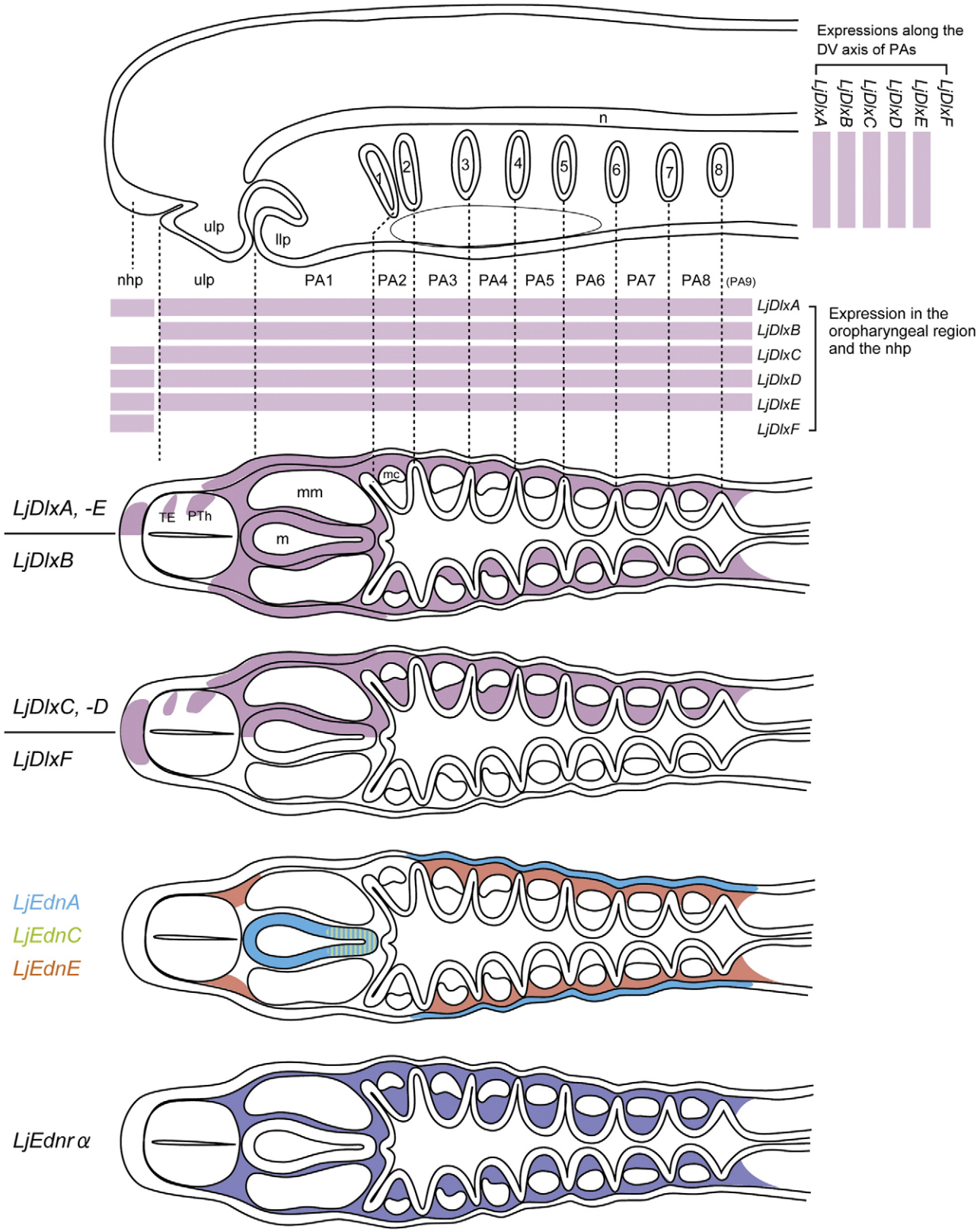

Fig. 6. Summary of craniofacial expression patterns of *Dlx*, *Edn*, and *Ednr* genes in lamprey embryos. Expression patterns of *L. japonicum Dlx* genes at stage 26 were shown as illustrations. Red vertical and horizontal bars show ranges of *Dlx* expressions observed in *in situ* hybridization. nhp, nasohypophysial (olfactory) placode; ulp, upper lip; lower, lip; PA, pharyngeal arch; TE, telencephalon; PTh, prethalamus; m, mouth; mc, mesodermal core; mm, mandibular mesoderm.

LjDlx gene, we prepared two riboprobes harboring separate cDNA stretches. Wherever possible, we followed this policy to confirm the specificity of expression signals with multiple non-overlapping riboprobes (see Supplementary Table 1 for details of the riboprobes). Protocols for *in situ* hybridization were described previously (Kuraku et al., 2005; Takio et al., 2007).

Acknowledgments

We are grateful to S. Hirano and R. Kusakabe for embryos of the Japanese lamprey and to K.G. Ota, Y. Murakami, H. Wada and T. Yao for their valuable discussion. This project was supported by Grants-in-Aid from the Ministry of Education, Science and Culture of Japan.

Appendix A. Supplementary data

Supplementary data associated with this article can be found, in the online version, at doi:10.1016/j.ydbio.2010.02.013.

References

Braasch, I., Volff, J.N., Schartl, M., 2009. The endothelin system: evolution of vertebrate-specific ligand–receptor interactions by three rounds of genome duplication. Mol. Biol. Evol. 26, 783–799.

Clouthier, D.E., Hosoda, K., Richardson, J.A., Williams, S.C., Yanagisawa, H., Kuwaki, T., Kumada, M., Hammer, R.E., Yanagisawa, M., 1998. Cranial and cardiac neural crest defects in endothelin-A receptor-deficient mice. Development 125, 813–824.

Debiais-Thibaud, M., Germon, I., Laurenti, P., Casane, D., Borday-Birraux, V., 2008. Low divergence in Dlx gene expression between dentitions of the medaka (Oryzias latipes) versus high level of expression shuffling in osteichtyans. Evol. Dev. 10, 464–476.

Depew, M.J., Lufkin, T., Rubenstein, J.L., 2002. Specification of jaw subdivisions by Dlx genes. Science 298, 381–385.

Guindon, S., Gascuel, O., 2003. A simple, fast, and accurate algorithm to estimate large phylogenies by maximum likelihood. Syst. Biol. 52, 696–704.

Holland, N.D., Holland, L.Z., Honma, Y., Fujii, T., 1993. Engrailed expression during development of a lamprey, Lampetra japonica: a possible clue to homologies between agnathan and gnathostome muscles of the mandibular arch. Dev. Growth Differ. 35, 153–160.

Hunt, P., Whiting, J., Nonchev, S., Sham, M.H., Marshall, H., Graham, A., Cook, M., Allemann, R., Rigby, P.W., Gulisano, M., et al., 1991. The branchial Hox code and its implications for gene regulation, patterning of the nervous system and head evolution. Development (Suppl 2), 63–77.

Hyndman, K.A., Miyamoto, M.M., Evans, D.H., 2009. Phylogeny, taxonomy, and evolution of the endothelin receptor gene family. Mol. Phylogenet. Evol. 52, 677–687.

Janvier, P., 1996. Early Vertebrates. Oxford University Press, New York, NY.

Kimmel, C.B., Ullmann, B., Walker, M., Miller, C.T., Crump, J.G., 2003. Endothelin 1-mediated regulation of pharyngeal bone development in zebrafish. Development 130, 1339–1351.

Koentges, G., Matsuoka, T., 2002. Evolution. Jaws of the fates. Science 298, 371–373.

Kuraku, S., 2008. Insights into cyclostome phylogenomics: pre-2R or post-2R? Zool. Sci. 25, 960–968.

Kuraku, S., Usuda, R., Kuratani, S., 2005. Comprehensive survey of carapacial ridge-specific genes in turtle implies co-option of some regulatory genes in carapace evolution. Evol. Dev. 7, 3–17.

Kuraku, S., Takio, Y., Tamura, K., Aono, H., Meyer, A., Kuratani, S., 2008. Noncanonical role of Hox14 revealed by its expression patterns in lamprey and shark. Proc. Natl. Acad. Sci. U. S. A. 105, 6679–6683.

Kuraku, S., Meyer, A., Kuratani, S., 2009. Timing of genome duplications relative to the origin of the vertebrates: did cyclostomes diverge before or after? Mol. Biol. Evol. 26, 47–59.

Kuratani, S., 2005. Developmental studies of the lamprey and hierarchical evolutionary steps towards the acquisition of the jaw. J. Anat. 207, 489–499.

Kuratani, S., Ota, K.G., 2008. Primitive versus derived traits in the developmental program of the vertebrate head: views from cyclostome developmental studies. J. Exp. Zoolog. B Mol. Dev. Evol. 310, 294–314.

Kuratani, S., Ueki, T., Aizawa, S., Hirano, S., 1997. Peripheral development of cranial nerves in a cyclostome, Lampetra japonica: morphological distribution of nerve branches and the vertebrate body plan. J. Comp. Neurol. 384, 483–500.

Kuratani, S., Nobusada, Y., Horigome, N., Shigetani, Y., 2001. Embryology of the lamprey and evolution of the vertebrate jaw: insights from molecular and developmental perspectives. Philos. Trans. R. Soc. Lond. B Biol. Sci. 356, 1615–1632.

Kuratani, S., Kuraku, S., Murakami, Y., 2002. Lamprey as an evo–devo model: lessons from comparative embryology and molecular phylogenetics. Genesis 34, 175–183.

Kurihara, Y., Kurihara, H., Suzuki, H., Kodama, T., Maemura, K., Nagai, R., Oda, H., Kuwaki, T., Cao, W.H., Kamada, N., et al., 1994. Elevated blood pressure and craniofacial abnormalities in mice deficient in endothelin-1. Nature 368, 703–710.

Kurihara, Y., Kurihara, H., Oda, H., Maemura, K., Nagai, R., Ishikawa, T., Yazaki, Y., 1995. Aortic arch malformations and ventricular septal defect in mice deficient in endothelin-1. J. Clin. Invest. 96, 293–300.

Larhammar, D., Lundin, L.G., Hallbook, F., 2002. The human Hox-bearing chromosome regions did arise by block or chromosome (or even genome) duplications. Genome Res. 12, 1910–1920.

Maemura, K., Kurihara, H., Kurihara, Y., Oda, H., Ishikawa, T., Copeland, N.G., Gilbert, D.J., Jenkins, N.A., Yazaki, Y., 1996. Sequence analysis, chromosomal location, and developmental expression of the mouse preproendothelin-1 gene. Genomics 31, 177–184.

Mallatt, J., 2008. The origin of the vertebrate jaw: neoclassical ideas versus newer, development-based ideas. Zool. Sci. 25, 990–998.

Miller, C.T., Yelon, D., Stainier, D.Y., Kimmel, C.B., 2003. Two endothelin 1 effectors, hand2 and bapx1, pattern ventral pharyngeal cartilage and the jaw joint. Development 130, 1353–1365.

Moore, W.J., 1981. The Mammalian Skull. Cambridge Univ. Press, London.

Murakami, Y., Ogasawara, M., Sugahara, F., Hirano, S., Satoh, N., Kuratani, S., 2001. Identification and expression of the lamprey Pax6 gene: evolutionary origin of the segmented brain of vertebrates. Development 128, 3521–3531.

Myojin, M., Ueki, T., Sugahara, F., Murakami, Y., Shigetani, Y., Aizawa, S., Hirano, S., Kuratani, S., 2001. Isolation of Dlx and Emx gene cognates in an agnathan species, Lampetra japonica, and their expression patterns during embryonic and larval development: conserved and diversified regulatory patterns of homeobox genes in vertebrate head evolution. J. Exp. Zool. 291, 68–84.

Nataf, V., Lecoin, L., Eichmann, A., Le Douarin, N.M., 1996. Endothelin-B receptor is expressed by neural crest cells in the avian embryo. Proc. Natl. Acad. Sci. U. S. A. 93, 9645–9650.

Neidert, A.H., Virupannavar, V., Hooker, G.W., Langeland, J.A., 2001. Lamprey *Dlx* genes and early vertebrate evolution. Proc. Natl. Acad. Sci. U. S. A. 98, 1665–1670.

Ota, K.G., Kuraku, S., Kuratani, S., 2007. Hagfish embryology with reference to the evolution of the neural crest. Nature 446, 672–675.

Panganiban, G., Rubenstein, J.L., 2002. Developmental functions of the Distal-less/Dlx homeobox genes. Development 129, 4371–4386.

Rijli, F.M., Mark, M., Lakkaraju, S., Dierich, A., Dolle, P., Chambon, P., 1993. A homeotic transformation is generated in the rostral branchial region of the head by disruption of Hoxa-2, which acts as a selector gene. Cell 75, 1333–1349.

Sato, T., Kurihara, Y., Asai, R., Kawamura, Y., Tonami, K., Uchijima, Y., Heude, E., Ekker, M., Levi, G., Kurihara, H., 2008. An endothelin-1 switch specifies maxillomandibular identity. Proc. Natl. Acad. Sci. U. S. A. 105, 18806–18811.

Shigetani, Y., Sugahara, F., Kawakami, Y., Murakami, Y., Hirano, S., Kuratani, S., 2002. Heterotopic shift of epithelial–mesenchymal interactions in vertebrate jaw evolution. Science 296, 1316–1319.

Shigetani, Y., Sugahara, F., Kuratani, S., 2005. A new evolutionary scenario for the vertebrate jaw. Bioessays 27, 331–338.

Stock, D.W., 2005. The Dlx gene complement of the leopard shark, Triakis semifasciata, resembles that of mammals: implications for genomic and morphological evolution of jawed vertebrates. Genetics 169, 807–817.

Stock, D.W., Ellies, D.L., Zhao, Z., Ekker, M., Ruddle, F.H., Weiss, K.M., 1996. The evolution of the vertebrate Dlx gene family. Proc. Natl. Acad. Sci. U. S. A. 93, 10858–10863.

Tahara, Y., 1988. Nomal staging of development in the lamprey, *Lampetra reissneri* (Dybowski). Zool. Sci. 5, 109–118.

Takio, Y., Pasqualetti, M., Kuraku, S., Hirano, S., Rijli, F.M., Kuratani, S., 2004. Evolutionary biology: lamprey Hox genes and the evolution of jaws. Nature 429 1 p following 262.

Takio, Y., Kuraku, S., Murakami, Y., Pasqualetti, M., Rijli, F.M., Narita, Y., Kuratani, S., Kusakabe, R., 2007. Hox gene expression patterns in *Lethenteron japonicum* embryos-insights into the evolution of the vertebrate Hox code. Dev. Biol. 308, 606–620.

Thomas, A.J., Erickson, C.A., 2008. The making of a melanocyte: the specification of melanoblasts from the neural crest. Pigment Cell Melanoma Res. 21, 598–610.

Venkatesh, B., Kirkness, E.F., Loh, Y.H., Halpern, A.L., Lee, A.P., Johnson, J., Dandona, N., Viswanathan, L.D., Tay, A., Venter, J.C., Strausberg, R.L., Brenner, S., 2007. Survey sequencing and comparative analysis of the elephant shark (*Callorhinchus milii*) genome. PLoS Biol. 5, e101.

Wilson, J., Tucker, A.S., 2004. Fgf and Bmp signals repress the expression of Bapx1 in the mandibular mesenchyme and control the position of the developing jaw joint. Dev. Biol. 266, 138–150.

Wotton, K.R., Weierud, F.K., Dietrich, S., Lewis, K.E., 2008. Comparative genomics of Lbx loci reveals conservation of identical Lbx ohnologs in bony vertebrates. BMC Evol. Biol. 8, 171.

Yalden, D.W., 1985. Feeding mechanisms as evidence for cyclosome monophyly. Zool. J. Linn. Soc. 84, 291–300.

Yao, T., Ohtani, K., Wada, H., 2008. Whole-mount observation of pharyngeal and trabecular cartilage development in lampreys. Zool. Sci. 25, 976–981.